



Electronic Properties of Nano- and Submicron Semiconductor Particle Layers

Nikolay D. Zhukov , Mikhail I. Shishkin , Ildar T. Yagudin, Aleksander A. Khazanov, Maksim V. Gavrikov

For citation:

Zhukov N. D., Shishkin M. I., Yagudin I. T., Khazanov A. A., Gavrikov M. V. Electronic Properties of Nano- and Submicron Semiconductor Particle Layers. *Scientific Research and Innovation*. 2020;1(1):22-30 DOI:10.34986/MAKAO.2020.95.51.005

Authors' credentials:

Nikolay D. Zhukov, Candidate of Physics&Mathematics, Director, Ref-Volga-Svet LLC, 101, 50 Let Oktyabrya St., Saratov, 410033, RF.

Mikhail I. Shishkin, Candidate of Physics&Mathematics, Senior Lecturer, Chair of Semiconductor Physics, Saratov State University, 83 Astrakhanskaya St., Saratov, 410012, RF. (shishkin1mikhail@gmail.com)

Maksim V. Gavrikov, Postgraduate Student, Chair of Semiconductor Physics, Saratov State University, 83 Astrakhanskaya St., Saratov, 410012, RF.

Ildar T. Yagudin, Research Scientist, Ref-Volga-Svet LLC, 101, 50 Let Oktyabrya St., Saratov, 410033, RF.

Aleksander A. Khazanov, Research Scientist, Ref-Volga-Svet LLC, 101, 50 Let Oktyabrya St., Saratov, 410033, RF.

Competing interests:

The authors declare no competing interests.

Acknowledgements: The research received RFBR's financial support within the framework of research projects 17-07-00139 a and 18-37-00085 mol_a.

Received: 20 December 2019

Revised: 2 February 2020

Accepted: 12 March 2020

Published: 15 April 2020

Abstract: Studying multigrain layers (MGL) formed by nanoparticles of Si, GaAs, InAs, InSb semiconductors and CdSe and PbS colloidal quantum dots (CQDs) reveals that the current-voltage curves for InAs, GaAs and Si MGL and PbS CQDs are determined by nanoparticles' tunneling from near-surface electron states. In the case of Si tunneling is replaced by thermionic emission when the temperature and voltage increase. For the CdSe CQD MGL the current-voltage curve is almost linear. Evaluation of the current-voltage curves with gradual to-and-fro voltage alteration revealed a hysteresis-type effect which can be attributed to the intergranular electron charge exchange. The PbS QD photoconductivity range was found to contain dark current suppression with maximum values within the wavelength range of 1600–2500 nm, which can be caused by impurity electron levels related to oxygen. Such effects, indicative of photomemory occurring due to charge-carrier injection into MGL, can be utilized in photoluminescent or electroluminescent LEDs. Elaboration of CdSe and PbS nanoparticle self-arrangement mechanism enabled us to design a light source with multichannel element radiation spectrum control, which can be used for non-invasive biomedical quick testing. Multigrain structures are expected to be used in making such optoelectronic devices as solar cells and memory cells.

Keywords: quantum dots, semiconductor nanoparticles, powders, multigrain structure, tunneling transmission, luminescence, hysteresis, conductivity submission, thermionic emission.

Semiconductor nanoparticles including those quantum-dimensional (quantum dots or QD) and the structures which they form constitute an important nanotechnology issue and are used in medicine for luminescent visualizing of cell structures [1,2]. An important task related to the synthesis, technology, research and application of semiconductor nanoparticles is the controlled arranging of nanoparticles into structured assemblies serving as functional elements in building of optoelectronics and photovoltaic devices featuring unusual electronic properties due to cooperative electronic effects [3]. The simplest but most technically viable option thereof consists in the self-arrangement of nanoparticles on a substrate into a thin-film layer [4]. Structures of this kind can be called multigrain structures (MGS) by analogy with metals [5]. The electrophysical and optical properties of such structures depend on the material, size, shape and density of the nanograin crystallites, the degree of their contact and the medium

filling the intergranular space. Such structures can be used in gas and optical sensors, receivers and sources of infrared radiation, or solar inverters.

MGSs belong to random structures, whereof the best studied ones are polycrystalline semiconductors. Multiple publications concerning polycrystalline materials dwell upon densely packed structures with virtually non-existent spacing between nanograin crystallites. They are treated within the physical models of grain boundary electron scattering (for metals) or contact phenomena (for semiconductors). The distinctive feature of the MGS studied in this research is the relatively large spacing between the grains supporting the electrons' emission from the grains into the spacing and injection from the spacing into the grains. We investigated these processes by studying individual grains by scanning tunnel microscopy [6-9].

Examination of the electric current mechanics in the semiconducting MGSs which appear most advantageous for implementation, such as Si, GaAs, InAs and InSb, revealed that their behavior is conditioned by the mechanism of intergranular tunnel emission from the submicron particles' surface electronic states. We have found out the emission parameters. We obtained the current (I) on voltage (V) dependence formula (the current-voltage curve):

$$I/I_0 \sim \exp(-B_0 ZN/V), \quad (1)$$

Where: $B_0 \sim 3.5(m/m_0)^{1/2} \psi^{3/2}$; ψ [eV] stands for the value of the barrier for the electrons emitted from the nanoparticles; m/m_0 signifies the effective electron mass in semiconductor; Z [nm] denotes the average interparticle spacing size and N designates the average number of conducting interparticle spacings along the current flow line (through-thickness direction).

A lot of promise is demonstrated by narrow-band-gap semiconductors embodying favorable conditions for manifestation of collective electronic effects [6,10].

The procedures of this research included a number of process studies and continued examination of current flow mechanics, as well as the photoelectric properties of nanoparticle (and quantum dot) MGSs of the Si, GaAs, InAs, InSb, CdSe, PbS semiconductor group obtained in the laboratories

of Saratov State University, *Ref-Svet* LLC (Saratov, Russia) and Research Institute of Applied Acoustics (Dubna, Russia).

Materials and Research Methods

In this study, we used submicron particles of single-crystal semiconductors Si, GaAs, InAs and InSb, made by mechanical grinding in compliance with [11], and colloidal quantum dots (QDs) of CdSe and PbS semiconductors obtained by colloidal synthesis [12]. Nanoparticles were deposited by electrophoresis from suspensions in a thin cell [9] and by self-arrangement of assemblies on the surface during controlled evaporation of the solvent [4].

Self-arrangement and self-assembly in a droplet or thin film imply a limited timespan evolution of the system from the initial state, when the elements of the system enjoy mobility, to the final one, wherein the elements lose mobility, forming the final morphology characterized by nanoparticle assembly structural rigidity.

The initial suspension was made with isopropyl alcohol which was chosen experimentally as the most appropriate solvent. The solution's optimal particle concentration was estimated at 2 g per 40 ml.

Electrophoretic precipitation was ensured by adding 1 ml of the charger $[\text{Al}(\text{NO}_3)_3 + \text{La}(\text{NO}_3)_3]$ 0.1 M water solution and 0.3 ml of the dispersant (glycerine). The suspension was treated with an ultrasound-emitting immersion probe alongside with constant stirring for three hours. During the particles' precipitation the substrate acted as the cathode and was positioned horizontally above the bath bottom covered with a conductive layer of ITO and acting as the anode, the anode-to-cathode distance being 0.5 mm. The precipitation was performed for 1 min at 15 VDC. Upon completing precipitation the sample was rinsed with acetone and air-dried at 120 °C.

The multigrain layer nanoparticle size and structure was monitored using scanning electronic (SEM) microscopy and tunneling (STM) microscopy [11].

The procedure yielded 3D nanostructure assemblies with multilayer morphology. The SEM and STM visualization of typical experiment results are shown in Figure 1 (GaAs, most particles not exceeding 100 nm). Comparison between the two

above-described procedural approaches revealed that the denser particle layer packing was yielded by cataphoretic deposition.

Substrate deposition of colloid quantum dots features certain peculiarities due to the relatively high viscosity of the suspension stabilizer which prevents the particles from sticking together but renders the deposited layer uneven. This issue was addressed by replacing the stabilizer with ethanol immediately prior to commencing the deposition. The latter was accomplished by multiple mixing of the initial suspension with an adjusted proportion of ethanol in an Eppendorf tube with their subsequent centrifuge separation.

The MGS current flow mechanics was examined by performing the analysis of the current-voltage curves obtained by the procedures described in the paper [9]. One of the problems encountered during current-voltage curve analysis is that of ohmic contacts with the MGS. In earlier research this issue was addressed by studying the contact resistance using both the researcher's own data and those obtained from literature [13]. Supplementary to the earlier implemented examination methods [9] this research used electron beam vacuum tubes. The samples constituted an anode-grid-cathode triode with the flat anode being covered with the MGS. The sample's single substrate located all the types of the studied materials and the test element for current-voltage curve monitoring of the system formed by the grid and MGS-electrode. The test element voltage drop values were estimated in relation to the sample voltage values for each of the measured current values. This facilitated estimation of the MGS voltage drop values and, respectively, drawing of the MGS current-voltage curves. Another advantage of the vacuum method implementation was that it provided the opportunity of studying the temperature dependencies of the current-voltage curves by protecting the current-voltage curves from the atmospheric impact which was registered and required compensating measures during open-air measurements.

The photoelectric properties were studied using a spectrometric modification of MDR-41 monochromator with replaceable diffraction grating. The photoconductivity evaluation circuit diagram included a direct-current power supply, the sample and a 300 k Ω load resistor placed at the output

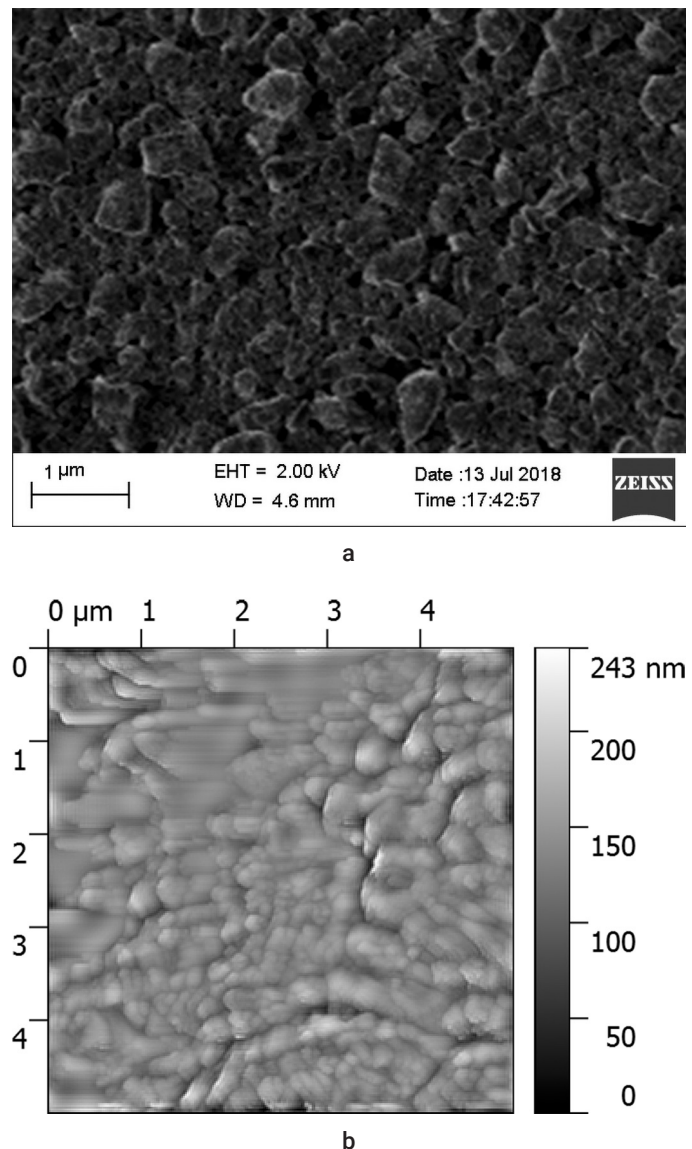


Figure 1. Multigrain layer SEM (a) and STM (b) images

analog-to-digital converter from which the signal was picked up. The light was emitted by a halogen lamp, passed through a light filter and then through the monochromator, its spectrum being scanned at 70 nm/min with the scanning pitch determined by the diffraction grating resolution.

Current Flow Mechanisms

The MGS conductivity is determined by the linear current circuit intergranular processes [9, 14], among which three current flow mechanisms are possible, namely the ohmic one through direct particle contacts, the tunneling and thermionic emission. The current-voltage curve demonstrates the features of the rate-controlling process. It is obvious

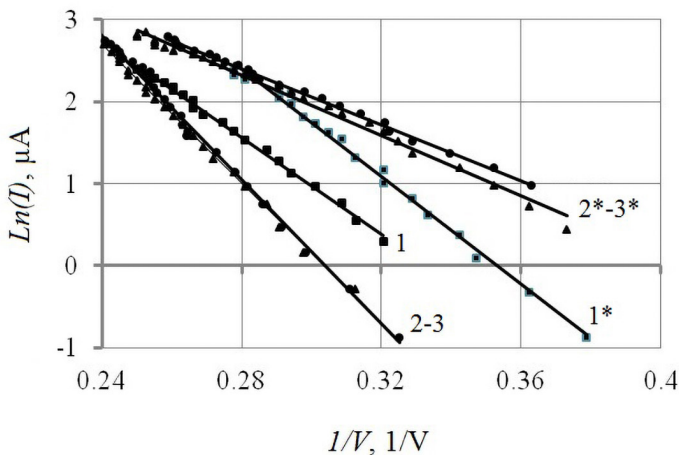


Figure 2. Current-voltage for InAs (1, 2, 3) and GaAs (1*, 2*, 3*) samples at different temperatures: 1, 1* – 295 K; 2, 2* – 333 K; 3, 3* – 383 K

that the electrons are transported from the surface grain layer which features the thickness comparable with the de Broglie wavelength of an electron, which in case of the studied semiconductors may be as large as dozens of crystalline monolayers.

The ohmic contact was not studied in this research as the current-voltage curves of the structures examined herein are conspicuously non-linear, whereas the evaluation of the contact resistance values is unfavorable towards the ohmic mechanisms version as well [9, 13, 14]. The current-voltage curves for the tunneling and thermionic emission demonstrate exponential dependence described, respectively, by formulas $I \sim A \exp[B/V]$ и $I \sim A \exp[BV]$. Another typical feature of such processes is the $B \sim T$ temperature dependence, which is weak for tunneling and strong for emission.

MGS with Submicron Particles

Examination of the current-voltage curves for the InAs and GaAs samples revealed that in all the cases the $I \sim A \exp[B/V]$ dependence tunneling character manifestation featured high approximation reliability value $R^2 \sim (0.9913-0.9972)$. On the contrary, the dependencies of the $I \sim A \exp[BV]$ type had an unacceptable level of R^2 value at 0.92–0.96.

Figure 2 shows the current-voltage curves for different temperatures. They reveal the B value's weak temperature dependence of temperature T . It is also notable that temperature growth decreases

the value of current for the narrow-bandgap InAs while increasing it for the wide-gap GaAs. This can be explained by the impact which the electron concentration level has on such tunneling parameters as mobility (effective mass) and work function. The rise in temperature triggers a certain growth of the conductivity electron concentration in the narrow-bandgap InAs, decrease of their mobility (the effective mass increasing), while the work function remains almost the same [15].

This results in decreasing tunneling probability and, respectively, current values. As for GaAs, the temperature increase causes a significant growth of conductivity electron concentration and, respectively, change in Fermi characteristic energy level thus bringing about a drop in work function entailing increase of the current values. The current-voltage curves parameters do not demonstrate significant changes.

Figure 3 demonstrates the Si MGS current-voltage curves in coordinates $\ln I \sim 1/V$ (a) and $\ln I \sim V$ (b). At the temperatures 295 K and 333 K for voltage value being $V > 5V$ the current-voltage curves can be efficiently ($R^2 > 0.995$) approximated by tunneling mechanism dependency and by the thermionic one for 333 K at $V < 5V$ or for 383 K at any V value.

In all the examined cases the tunneling and thermionic emission are competitive: the rise of temperature facilitates thermal emission while the voltage growth causes tunneling (provided that the surface particle layer of the semiconductors with n-type conductivity is electron-rich and the voltage polarity plus is on the n-type sample). The A_3B_5 semiconductor varieties are different from silicon in that their electron mobility exceeds that of the latter almost ten-fold which implies a lower effective mass. It results in a much higher tunneling probability. Therefore in all the cases regardless of the temperature and voltage values InAs and GaAs steadily manifest tunneling with such recognizable I-V curve properties as $\ln I \sim B/V$ and weak $B \sim T$ temperature dependence. Unlike that, in silicon tunneling is manifested at a higher voltage and relatively low temperatures.

Quantum Dot MGS

The research [10] studied the current-voltage curves of the MGS with submicron-size semiconducting particles with the dimensions ranging between 0.1

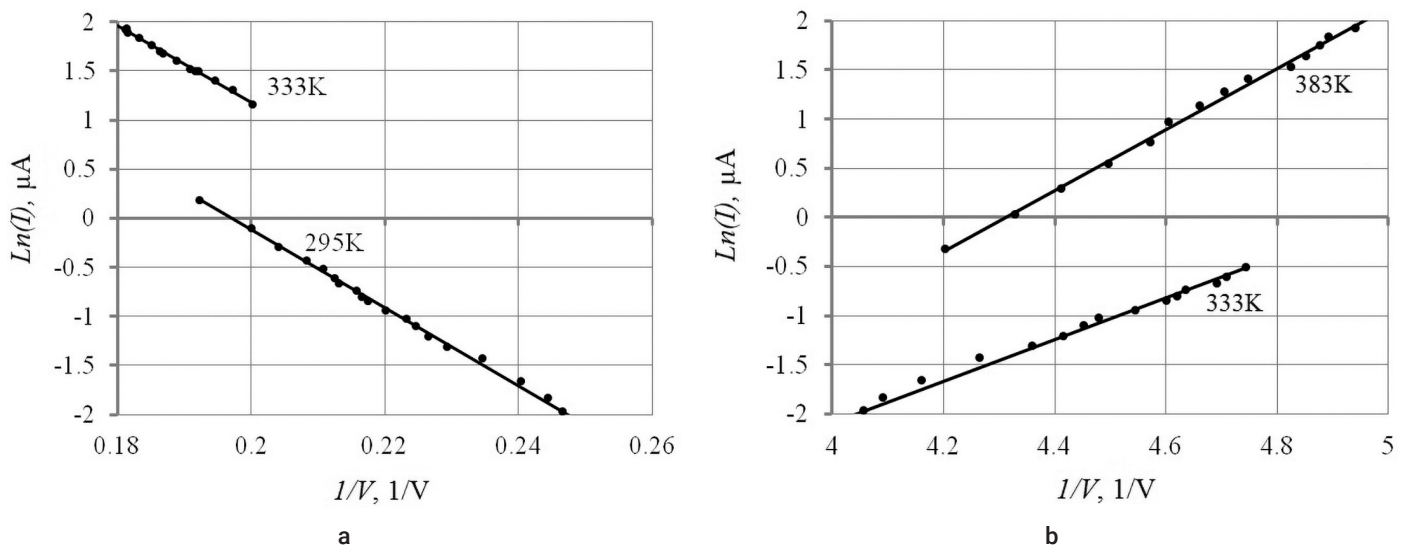


Figure 3. Si MGS current-voltage curves for different temperatures in the reference axes for (a) tunneling and (b) thermionic emission

and 11 μm. It was found out that the current-voltage curves follow formula (1). We found the values of B_0 and NZ , as well as that of the emission clearance threshold field intensity E_{n^*} :

B_0 (V/nm):
for InSb ~ 2.5; InAs ~ 4.0; GaAs ~ 5.0; Si ~ 12.

NZ (nm)
V for InSb ~ 50; InAs ~ 30; GaAs ~ 15, Si ~ 5.

E_n (V/cm):
for InSb ~ $4 \cdot 10^6$; InAs ~ $6 \cdot 10^6$; GaAs ~ $8 \cdot 10^6$; Si ~ $2 \cdot 10^7$.

This research has examined the I-V curves for colloid quantum dot MGS. Figure 4 demonstrates the current-voltage curves for PbS and CdSe QD MGS with 2–5 nm quantum dots. The PbS QD MGL I-V curve can be efficiently approximated under formula (1) within the entire measurement range at $B_0NZ \sim 17$ [B] (Figure 4a).

Such approximation cannot be performed for the CdSe QD MGS while its current-voltage curve is almost linear. At a separate I-V curve section formula (1) approximation can be performed within a limited range at $B_0NZ \sim 1.5$ [B] (Figure 4b).

The small B_0NZ values found when dealing with quantum dots can signify that the values $B_0 \sim 3.5 (m/m_0)^{1/2} \psi^{3/2}$ are extremely small for them, so establishing of $m/m_0 \sim (0.05-0.1)$ and $NZ \sim 10$ can render the

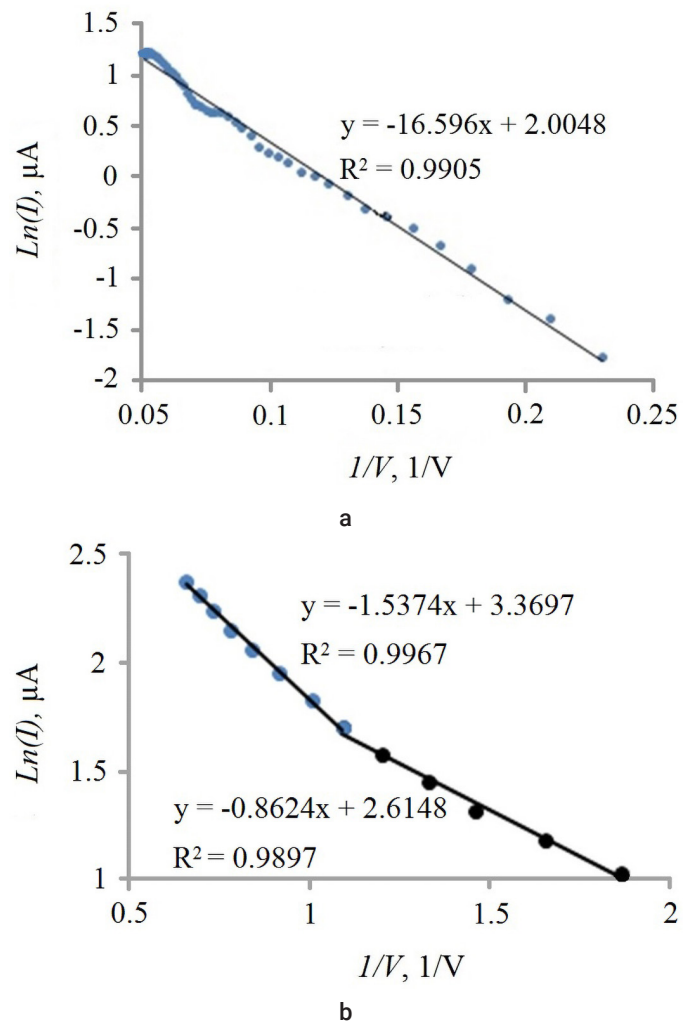


Figure 4. PbS (a) and CdSe (b) quantum dot MGS current-voltage curves

ψ value well below one eV, which is much lower than the studied semiconductors' work function value.

Hysteresis of the current-voltage curves

Conductivity kinetics and nonstationary effects observed in random structures including multigrain ones are important features of the latter [14].

Evaluation of the current-voltage curves with gradual application of voltage from minus to plus and vice versa revealed a faint hysteresis-type effect which can be attributed to the delayed intergranular electron charge exchange and the charge-limited current (the difference of currents in the current-voltage curve being negative) during the transition of electron between the MGS grains by tunneling emission. Illumination intensified manifestation of hysteresis. Figure 5 specifies the respective values of the current-voltage curve difference during to-and-fro voltage scanning. The current-voltage curves voltage difference was positive under illumination which can be explained by the emission current growth due to the grain electron concentration increase by band-to-band transition and conductivity electrons energy increase facilitating their overcoming of the tunneling and emission barriers. Scanning of the voltage application mode performed within examination of the current-voltage curves revealed their unstable behavior which can be attributed to the unstable duration of the intergranular spacing charge exchange due to switching between the parallel current channels.

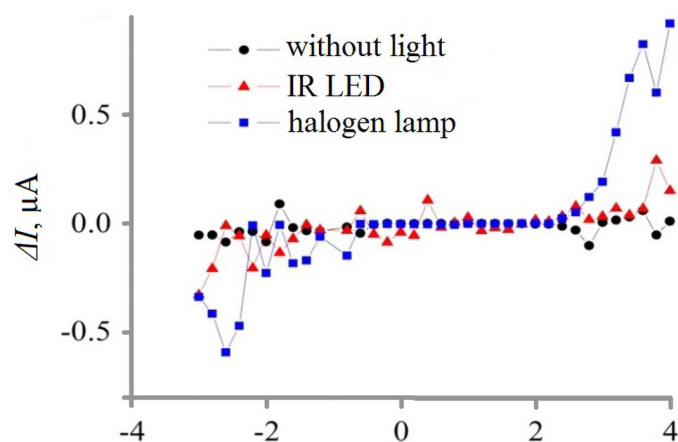


Figure 5. Typical diagram for GaAs particle MGS current-voltage curve relative current difference in darkness and when exposed to light

Optoelectronic Properties of the PbS and CdSe MGS

So far practical application of semiconducting nanoparticles including quantum-sized ones (colloid quantum dots) is confined to acting as phosphors in LEDs and highlighters. 'Traditional' instrumental applications are limited by the lack of reliable structures among those most practically expedient whereof the broadest applicability is demonstrated by the layer-upon-substrate structure. The latter's application in instruments requires further studies similar to the present one.

An important peculiarity of the semiconducting nanoparticle instrumental application philosophy is the possible usage of substrates featuring complicated (three-dimensional) structure such as a bulk-porous one like porous silicon or multichannel one like glass. As it was shown by the analysis, structures of this kind can serve the baseline for development of solar cells, image intensifiers or specialized light sources. These opportunities are being studied by the authors of this research.

Photoconductivity

Photoconductivity is an important parameter of film structures and its research can yield most promising results when involving the films with varied micro- and nanostructure [16]. The most notable manifestations of changes in structure and photoelectric properties can be found in nanostructured PbS [17] due to the narrow range of the dimensional distribution of its individual grains, as well as to its layer photoconductivity mechanics being conditioned mainly by changing concentration of non-equilibrium carriers in separate quantum dots [18]. Meanwhile the conductivity of nanopowder MGS is conditioned mainly by free carriers' energy growth caused by electric field application and is not strongly affected by illumination.

In this research the PbS quantum dots were deposited upon a glass substrate with film aluminum contacts to form a layer similar to a thin film produced by chemical precipitation [19], as demonstrated in Figure 6a. When connected to an electric circuit the deposited QD layer provided photoresistance, its photosensitivity range (as can be seen in Figure 6b) being dependent on the supplied voltage value (5 and 10 V). The sample's photosensitivity ranged within 500–1500 nm with a discernible peak value at 1100 nm thus notably differing from the sensitivity

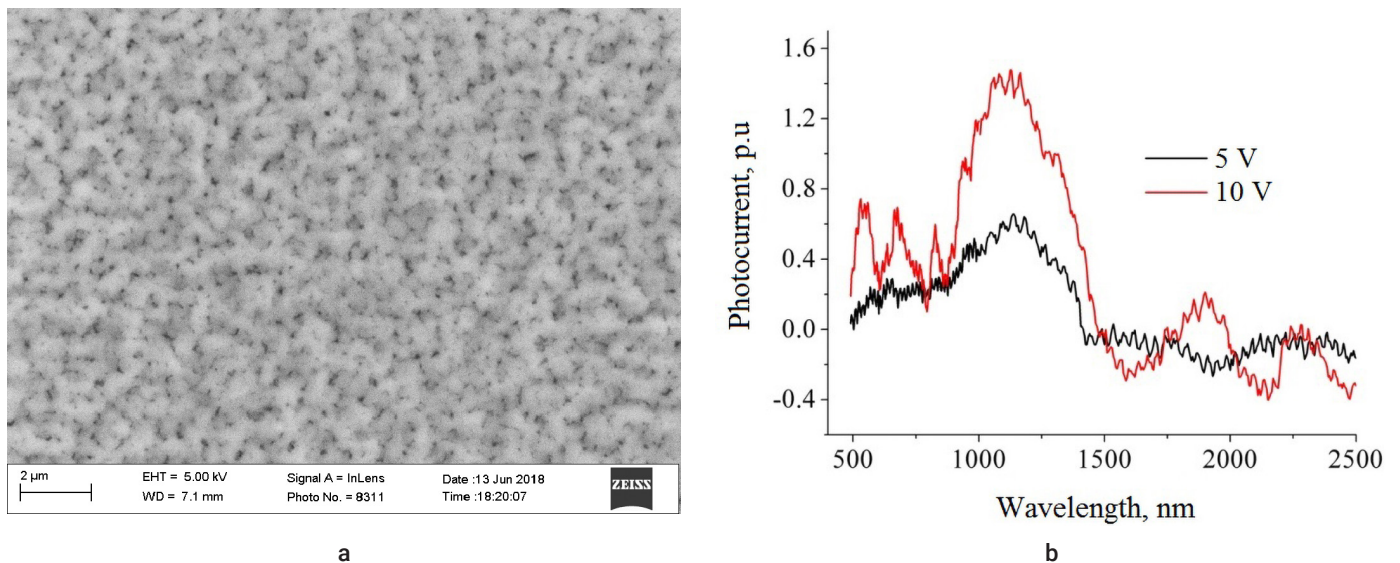


Figure 6. PbS QD layer (a) morphology electronic microscope image and (b) photoconductivity range

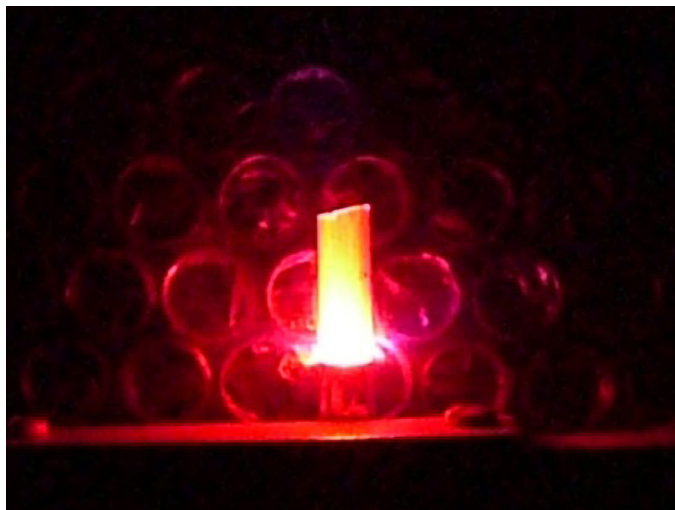


Figure 7. Output glow of CdS/CdSe QD MGS excited by violet LED

of conventional polycrystalline PbS photoresistors with the principal photosensitivity range of 1500–3000 nm [20]. It is remarkable that at wavelengths exceeding 1500 nm the signal was virtually always weaker than in darkness (achieving maximum values at ~1600, 2200, 2500 nm, see Figure 6) and changed from one measurement to another which can indicate processes similar to dark conductivity suppression. This can be brought about by impurity electron levels related to oxygen. With a higher supplied voltage the photocurrent peak values were registered in the shortwave part at 550, 670 and

820 nm of approximately the same width. There is no exhaustive explanation for these peaks though in the papers dwelling upon deposition of PbS QD layers by electrophysical and optical methods similar peaks were found in the absorption spectrum [21] and that of the solar cells' external quantum efficiency [22], which the authors attributed, respectively, either to the QD electron structure or with the ligands and the dissolvent.

It is evident that within the studied model of intergranular electron transport the MGS photoconductivity and its spectral dependence are determined by ways of the light affecting electron emission which include photoemission and light-induced field emission and tunneling emission from the surface grain level electron states. This vision requires a separate systematic research.

Photoluminescence

This one can be illustrated by the preliminary results yielded by the efforts aimed at developing a multi-channel structure quantum dot light source with a number of separately controlled spectral bands [23]. In order to form a light source the quantum dots of different semiconductors have to be arranged in such a way that the QD with a longer luminescence wavelength band would be placed closer to the multichannel structure's center so that their luminescence could pass through the QD having higher-energy radiation quanta without getting absorbed by them. Thus multichannel structure can serve the

framework for building a multiband spectral light source by depositing quantum dots of different types in a definite combination either simultaneously through a specially designed ‘mask’ on one of the flat ends or by building the source from separate microchannels which have their surfaces covered with QD of different semiconductors.

Figure 7 demonstrates the output glow emitted by a multichannel element with CdSe (2–3 nm) and PbS (4–5 nm) quantum dots when excited by a violet LED. An OS-17 optical filter was used to completely block the exciting violet radiation. The research is still in progress involving QD of various composition featuring high quantum efficiency to ensure a broader spectrum range.

Results

Analysis of the current–voltage curves reveals that their behavior for InAs and GaAs within the

temperature range $T = (295–383)$ K and Si (333 K) for voltage $V > 5$ V and 295 K for the entire V measurement range is determined by intergranular tunneling emission from surface electronic nanoparticle states, and by thermionic emission for Si ($T = 333$ K at $V > 5$ V and $T = 383$ K). The PbS QDs MGS are efficiently approximated by tunneling. The CdSe QDs MGS defies such approximation while the current–voltage curve itself is almost linear. Evaluation of the current–voltage curves with gradual to-and-fro voltage alteration revealed a hysteresis-type effect which can be attributed to the intergranular electron charge exchange and the charge-limited current. The PbS QD photoconductivity range was found to contain peak photoconductivity at 550, 670 and 820 nm and dark current suppression with maximum values $\sim 1600, 2200, 2500$ nm. Multigrain structures can be used in making such optoelectronic devices as solar cells, image intensifier tubes or light sources supporting spectrum control.

References

- Petrova E.A., Terpinskaya T.I., Artem'ev M.V., Ulashchik V.S. Semiconductor nanoparticles of cadmium selenide as fluorescent cell marker. *Doklady of the National Academy of Science of Belarus*. 2015;59(5):55–61. (In Russ.).
- Composite Media with Semiconductor Nanoparticles. Lektsii.com. 2019. [Retrieved October 30, 2019]. (In Russ.). Available at: <https://lektsii.com/1-153711.html>
- Vasil'ev R.B., Lazareva E.P., Putilin F.N., Ryabova L.I., Sokolikova M.S., Shlenskaya N.N. Quasi-bidimensional Semiconductor Nanoparticles and Their Assemblies: Synthesis, Optical and Electrophysical Properties. RFBR Grant Report 13-03-00760/13. Nomer TSITIS: 01201355994. [Retrieved October 30, 2019,]. (In Russ.). Available at: <https://istina.msu.ru/projects/5348321/>
- Adrianov V.E., Maslov V.G., Baranov A.V., Fedorov A.V., Artem'ev M.V. Spectral study of the self-organization of quantum dots during the evaporation of colloidal solutions. *Journal of Optical Technology*. 2011;78(11):699–705. DOI:10.1364/JOT.78.000699
- Ovcharenko V.E., Boyangin E.N., Ivanov K.V., Myshlyaev M.M., Ivanov Y.F. Formation of a multigrain structure and its influence on the strength and plasticity of the Ni_3Al intermetallic compound. *Physics of the Solid State*. 2015;57(7):1293–1299. DOI:10.1134/S1063783415070252
- Zhukov N.D., Gluhovskoy E.G., Mosiyash D.S. Local emission spectroscopy of surface micrograins in $A^{III}B^V$ semiconductors. *Semiconductors*. 2016;50(7):894–900. DOI:10.1134/S1063782616070265
- Zhukov N.D., Glukhovskoi E.G., Khazanov A.A. On the local injection of emitted electrons into micrograins on the surface of $A^{III}-B^V$ semiconductors. *Semiconductors*. 2016;50(6):756–760. DOI:10.1134/S1063782616060257
- Zhukov N. D., Kabanov V.F., Mihaylov M.I., Mosiyash D.S., Pereverzev Ya.E., Hazanov A.A., Shishkin M.I. Peculiarities of the Properties of III–V Semiconductors in a Multigrain Structure. *Semiconductors*. 2018;52(1):78–83. DOI:10.1134/S1063782618010256
- Zhukov N.D., Mosiyash D.S., Sinev I.V., Khazanov A.A., Smirnov A.V., Lapshin I.V.

- Mechanisms of Current Transfer in Electrodeposited Layers of Submicron Semiconductor Particles. *Technical Physics Letters*. 2017;43(12):1124-1127. DOI:10.1134/S106378501712029X
10. Zhukov N.D., Shishkin M.I., Rokakh A.G. Plasma Reflection in Multigrain Layers of Narrow-Bandgap Semiconductors. *Technical Physics Letters*. 2018;44:362-365. DOI:10.1134/S1063785018040284
11. Sinev I.V., Timoshenko D.A., Zhukov N.D., Sevostyanov V.P. Properties of Mechanically Dispersed Nano-Sized Single Crystals of III-V Semiconductors. *Nano- i Mikrosistemnaya Tekhnika*. 2018;20(8):475-480. DOI:10.17587/nmst.20
12. Dezhurov S.V., Rybakova A.V., Trifonov A.Y., Lovygin M.V., Krylsky D.V. Synthesis of highly photostable NIR-emitting quantum dots CdTeSe/CdS/CdZnS/ZnS. *Nanotechnologies in Russia*. 2016;11(5-6):337-343. DOI:10.1134/S199507801603006X
13. Blank T.V., Gol'dberg Yu.A. Mechanisms of current flow in metal-semiconductor ohmic contacts. *Semiconductors*. 2007;41(11):1263-1292. Mechanisms of current flow in metal-semiconductor ohmic contacts. DOI:10.1134/S1063782607110012
14. Kolosov S.A., Klevkov Yu.V., Plotnikov A.F. Electrical properties of fine-grained polycrystalline CdTe. *Semiconductors*. 2004;38(4):455-460. DOI:10.1134/1.173460
15. Madelung O., *Physics of III-V Compounds* (Mir, Moscow, 1967; Wiley, New York, 1964). 477 p.
16. Chernichkin V.I. Dobrovolsky A.A., Dashevsky Z.M. et al. Photoconductivity of PbTe:In films with variable microstructure. *Semiconductors*. 2011;45(11):1474-1478. DOI:10.1134/S1063782611110091
17. Sadovnikov S.I., Kozhevnikova N.S., Gusev A.I. Optical properties of nanostructured lead sulfide films with a DO_3 cubic structure. *Semiconductors*. 2011;45(12):1559-1570. DOI:10.1134/S1063782611120116
18. Konstantatos G. and Sargent Ed. H. PbS colloidal quantum dot photoconductive photodetectors: Transport, traps, and gain. *Applied Physics Letters*. *Appl. Phys. Lett.* 2007;91(17):173505-17505-3. DOI:10.1063/1.2800805
19. Markov V.F., Forostyanaya N.A., Ermakov A.N., Maskava L.N. Sintez tonkosloinykh tverdykh rastvorov v sisteme CdS-PbS metodom ionnogo zameshcheniya. [Hydrochemical synthesis of chalcogenide metal films. Part 12. Synthesis of thin-film solid solutions in the CdS-PbS system by ion-exchange substitution technique.] *Butlerov Communications = Butlerovskie soobshcheniya*. 2011;27(16):56-61. (In Russ.).
20. Mukhamed'yarov R.D., Miroshnikova I.N. Fotodetektory diapazona 0.2-3.8 μm na osnove sverkhchistykh plenok sulfida svintsa PbS i CdPbS. [PbS and CdPbS ultraclean film 0.2 to 3.8 μm wavelength range photodetectors.] *Sbornik dokladov kongressa "Ural Fotodetektory" = Ural Photodetectors Congress Book of Reports*. Ekaterinburg, 2017. p. 1-6. (In Russ.)
21. Konstantatos G. and Sargent E.H. Solution-Processed Quantum Dot Photodetectors. *Proceedings of the IEEE*. 2009;97(10):1666-1683. DOI:10.1109/JPROC.2009.2025612
22. Rongfang Wu, Yuehua Yang, Miaozi Li, Donghuan Qin, Yangdong Zhang and Lintao Hou. Solvent engineering for high-performance PbS quantum dots solar cells. *Nanomaterials*. 2017;7(8):201. DOI:10.3390/nano7080201
23. Zhukov N.D., Khazanov A.A., Shishkin M.I. Controlled Spectrum Light Source. RF Patent 2661441. Filed June 22, 2017. Held by "Ref-Svet" LLC.